Measurement of Doubly Charged Ions in Ion Thruster Plumes[*†]

George J. Williams, Jr.
The Ohio Aerospace Institute
NASA Glenn Research Center
MS-301-3, 21000 Brookpark Rd.
Cleveland, OH 44135
216-433-9622
george.j.williams@grc.nasa.gov

Matthew T. Domonkos
NASA Glenn Research Center
Cleveland, OH 44135

Joy M. Chavez
The University of Houston
Houston, TX 77004

IEPC-01-310

The ratio of doubly to singly charged ions was measured in the plumes of a 30 cm and of a 40 cm ion thruster. The measured ratio was correlated with observed erosion rates and thruster operating conditions. The measured and calculated erosion rates paralleled variation in the j^{++}/j^{+} ratio and indicated that the erosion was dominated by Xe III. Simple models of cathode potential surfaces which were developed in support of this work were in agreement with this conclusion and provided a predictive capability of the erosion given the ratio of doubly to singly charged ion currents.

Nomenclature

A_{SG}	Area of the screen electrode(cm^2)
$\underline{B}$	Magnetic field (G)
d	Electrode separation (m)
F	Flatness parameter
$\underline{E_p}$	Electric field (V/m)
E_I	Ion energy (eV)
$\underline{F}$	Force (N)
$f(E_I)$	Gaussian distribution (1/eV)
K	Arbitrary constant ($eV^{-3/2}$)
k	Boltzmann constant ($2.617 \cdot 10^{-8}$eV/k)
J	Current (A)
j	Current density (A/cm^2)
N	Number flux (s^{-1})
n	Number density (cm^{-3})
q	Ion charge state
R	Erosion rate (μm/khr)
r	Radial position (cm)
S_n	Energy conversion factor (eV)
T	Ion temperature (K)
V	Voltage (V)
v	Ion velocity (m/s)
y	Sputter yield (atoms/ion)
v_I	Ion velocity (m/s)
ϕ	Screen grid effective open area fraction
ν	Propellant utilization efficiency (uncorrected)
σ	Cross-section (m^2)
θ	Angle of incidence (deg)
ζ	Correction factor

Subscripts/Superscripts

B	Beam
D	Discharge
i	Ion
K	Keeper
P,PS	Pre-sheath
W	At the surface
+	Xe II ions
++	Xe III ions

[*]Presented as Paper IEPC-01-310 at the 27th International Electric Propulsion Conference, Pasadena, CA, 15-19 October, 2001.

Introduction

Ion thrusters are being scaled to different powers and operating conditions for space flight applications. Several wear-tests have been conducted to demonstrate long duration operation and determine life-limiting phenomena.[1,2,3] Potential failure mechanisms identified during these tests resulted from erosion of thruster components due to ion impact. Of particular interest to this investigation is the erosion of the discharge cathode assembly (DCA) and the screen electrode. These surfaces are at potentials on the order of the predicted sputtering threshold (~30 V). Screen grid and DCA erosion observed did not approach failure levels for these tests.[3] However, there is concern that at much higher thruster power levels or operation for much longer times erosion of these components might become mission threatening.[3]

The mechanisms behind the erosion process are currently under investigation.[4,5,6,7] Because of the relatively low potential fall expected at these surfaces, it is generally assumed that the erosion is due to doubly charged ions whose higher kinetic energy alone will result in orders of magnitude greater sputter yields.[3,7,11] However, laser-induced fluorescence (LIF) investigations have shown back-flowing Xe II ions near the face of the discharge cathode which may have sufficient energy to cause the observed erosion.[8] Whether Xe II contributes significantly to the erosion depends on the total ion density and the ratio of doubly to singly charged ions.

Several previous investigations have used an ExB mass spectrometer to measure the ratio of doubly to singly charged ions in the plumes of ion thrusters.[1,3,9,10] In these investigations, the doubly charged ion fraction was found to be proportional to discharge voltage and current.[1,9] The nature of the discharge voltage dependence indicated that the doubly charged ions result from sequential ionization.[9] However, it is unclear from these previous experiments that the variation in erosion recently observed in different wear tests resulted from different levels of doubly charged ion production.

In the present work presented here, an ExB mass spectrometer was used to measure the ratio of doubly charged to singly charged ion currents in the beams of two ion thrusters. Data were collected over a range of thruster operating conditions in order to identify those associated with a higher production of doubly charged ions. A correlation was then drawn between the production of doubly charged ions and the variation in observed discharge cathode assembly (DCA) erosion at similar conditions. To support this correlation, simple models of the erosion were used to predict the erosion rates and to identify the relative role of Xe II in the erosion process.

Apparatus and Procedure

Thrusters

A 30 cm engineering model thruster (EMT) and a 40 cm laboratory model thruster (LMT) were used in this investigation. The EMT was functionally identical to the flight model thruster currently operating on Deep Space 1[11] and the engine being used in the ongoing extended life test (ELT).[5] The LMT is a prototype, next-generation ion thruster.[12] The screen grid electrode used on both thrusters had the same open area fraction and grid hole geometry. The discharge chamber of the 40 cm thruster featured a larger plasma production volume, and a modified magnetic field that makes use of ferromagnetic structural material. These modifications led to preliminary indications that the flatness parameter of the 40 cm thruster was roughly fifty percent higher (i.e. flatter) than NSTAR.[11,13] The DCA in the 30 cm thruster was identical to that in the ELT thruster and similar to that used in the EMT's of the various wear tests. The DCA in the 40 cm thruster was a lab model assembly with twice the overall and orifice diameter of the one in the 30 cm thruster.

Table 1 gives the nominal thruster operating conditions investigated in this work. At these, discharge flow rates were varied to determine if small variations in the discharge voltage resulted in significant changes in the number of doubly charged ions.

Vacuum Facility

This investigation was performed in the Tank 11 vacuum test facility at GRC shown in Fig. 1. VF11 is 2.2 m in diameter by 9.0 m in length with four ports isolated with pneumatic gate valves. Four 0.9 m diameter and three 1.2 m diameter helium cryopumps yielded a pumping speed of approximately 240,000 liters per second (nitrogen). A 2-D motion control system drives a rake of electrostatic probes through the plasma plume. Resident optical diagnostics include CCD cameras and a 0.5 m

spectrometer for observation and spectroscopy, respectively.

ExB Probe

Figure 2a provides a schematic of the ExB mass spectrometer used in this investigation. This probe was used in an earlier investigation at GRC[1] during NASA Solar Electric Propulsion Technology Readiness (NSTAR) flight qualification testing. Additionally, the probe is identical to one currently being used at JPL for the Extended Life Test (ELT).[3,5]

The probe was fixed on thruster centerline 6.75 m downstream of the thruster. Because of its fixed location, data collected by the probe was not used to calculate plume divergence as in previous experiments.[9,10] The probe collected ions emitted from a strip across the diameter of the thruster roughly 4 cm wide as determined by the probe's acceptance angle. However, ions were preferentially collected from the center of this strip as illustrated in Fig. 2b.

The potential difference imposed across the probe deflection plates was supplied by two power supplies. Both supplies were controlled by a computer-based data collection system. The deflector electrodes were stepped in a bi-polar fashion. A picoammeter measured the ion current to the collector. At each step, four collector current readings were taken and averaged. Four consecutive sweeps of the probe were taken at each data point to quantify and reduce error.

The ExB probe measured the intercepted ion beam current associated with each ion charge state. Ions entering the probe were acted on by perpendicular electric and magnetic forces:

$$\underline{F} = q\underline{E_p} + q\underline{v_i} \times \underline{B}, \qquad (1)$$

where $E_p=V_p/d$. The magnetic field was generated by permanent magnets that deflected the ions toward the electrodes. The electric field was varied to counter this deflection until there was no net force acting on the ions. These ions which were not deflected then struck the collector at the rear of the probe. This process is illustrated in Fig. 2a. Since ion thrusters provide relatively mono-energetic ions for each charge state, singly and doubly charged ions were expected to be measured as well separated peaks.

Because the ExB probe collects ions in a distributed fashion across the diameter of the thruster, the measured j^{++}/j^{+} ratios are unknown-weighted averages which are not necessarily equal to those on centerline. A previous analysis compared ExB probe data integrated over radius and angle to simulate the current collection of the probe used in this investigation to data for centerline measurements. This analysis suggested a correction factor of 1.4 to approximate centerline j^{++}/j^{+} values. [14] This factor was based in part on the similarity between the flatness parameters of various thrusters. Although the 40 cm thruster has a higher flatness parameter, the same correction factor was used to approximate centerline ratios. In principle, a larger flatness parameter would decrease the radial variation in j^{++}/j^{+}. Therefore, the assumption of the same correction factor will yield a conservative estimate for erosion prediction.

Uncertainties in the ExB probe measurements included possibilities of internal and external probe misalignment. Internal misalignment included horizontal offsets of the collimating slits. These may result in shifts from the nominal $\sqrt{2}$ factor between the singles and doubles peaks and an increase in the width of the peaks associated with each current distribution. External, i.e. probe assembly, alignment was accomplished via laser sighting to the center of the thrusters. Since the collimating slits were in the vertical plane, slight vertical misalignment would have little impact on the measurement. However, horizontal misalignment could artificially reduce the j^{++}/j^{+} ratio.

Ideally, during a non-trivial segment of the deflector plate sweep, ion beam current should fully impact the collector yielding a "saturated" signal to ensure proper determination of peak current. However, the probe geometry permitted only a fraction of the ion beam to impact the collector at any given time. Although the probe did not permit saturation of the Xe II and Xe III current distributions, the j^{++}/j^{+} ratios were calculated from the peaks of each distribution.

Theory

Discharge Plasma Parameters

Xe III ions were assumed to be created preferentially in the primary regions of ionization in the discharge chamber. These regions were located in the plume of

the DCA and in the field-free region in the discharge chamber. In order to neglect the location of the Xe III production, the mean-free-path of charge-exchange collisions which would convert Xe III to Xe II ions should be significantly greater than the discharge chamber dimensions in which these collisions could occur.

The charge exchange cross section for Xe III-Xe I symmetric charge transfer (Xe III + Xe I $\rightarrow$ Xe I + Xe III) was roughly half that of Xe II-Xe I symmetric charge exchange cross-sections: 3 to $5 \cdot 10^{-15}$ cm^2 for 1 to 10 eV ion energies ($\sigma \propto 1/E_i$).[15] This cross-section was assumed to be equal to or greater than the non-resonant (Xe III + Xe I$\rightarrow$ 2Xe II) charge transfer.[15]

Xe II number densities in the discharge chamber were estimated to vary from 10^{13} cm^{-3} near the DCA[4] to 10^{10} to 10^{11} cm^{-3} at the grids based on current density calculations. The potential variation through the discharge chamber was assumed to be small implying the cross-section will be on the order of $5 \cdot 10^{-15}$ cm^2 throughout most of the chamber, The mean-free-path would then vary between 14 and 14,000 cm. LIF data indicated a two order of magnitude variation in density within the first 2 cm downstream of the DCA. Thus, the mean-free-path would vary between 1400 and 14000 cm throughout the vast majority of the chamber. It was unlikely that the Xe III ions would undergo charge exchange collisions before either impacting a surface or exiting the chamber. The variation in plasma density near the DCA also indicates a variation in plasma potential. Xe II ion velocities measured via LIF indicated that low-energy acceleration (1-10 eV) does take place within 1 to 2 cm of the DCA exit.[4,8]

Numerical Modeling

Simple numerical models of the erosion of cathode potential surfaces were developed to predict the erosion rates of these surfaces and to determine the relative contribution of Xe II to the erosion. The j^{++}/j^{+} ratio measured in the plume was assumed to be equal to that in the discharge chamber. Unequal Xe II and Xe III charge-exchange attenuation and divergence in the thruster plume were neglected.

DCA Erosion

A simple model of erosion due to Xe II and Xe III bombardment was developed to provide insight into the relative contributions of each in DCA erosion. The model included, where possible, LIF data for various DCA operating conditions and the erosion rates measured after the various wear tests.

At regular intervals across the radius of the DCA downstream surface, a Xe II bulk velocity and an angle of incidence were assumed along the downstream edge of the sheath of the keeper. These were measured for various operating conditions via LIF.[4,16] Xe III was assumed to have twice the energy and to be entering the sheath at the same angle. The ion temperatures were assumed to be equal for Xe II and Xe III and normalized Maxwellian velocity distributions were calculated about the bulk velocity of both Xe II and Xe III. Maxwellian velocity distributions were used rather than measured Xe II velocity distributions in order to simplify the model and to facilitate incorporation of bulk velocities different from those measured. The pre-sheath energy distributions were then calculated directly from these velocity distributions. Note, "ion temperature" is used here and below as a relative figure of merit to describe the spread in ion energies or velocities (which could be roughly approximated by a Maxwellian.[16] Local thermodynamic equilibrium (LTE) was not assumed to be present in the plasma.

A voltage drop, V_S, equal to $V_D - V_K$ is assumed across the sheath which will have a thickness of a few micrometers. Ions were accelerated through the sheath until they have gained the energy of the sheath in the direction normal to the sheath/surface:

$$E_{i,W} = E_{i,P} + qV_S \qquad (2)$$

The ions will then strike the DCA surface with an angle smaller than that with which they entered the sheath:

$$\theta_W = \tan^{-1}\left[\frac{v_i \sin(\theta)}{\left[\left(v_i \cos(\theta)\right)^2 + \frac{2qV_s}{m}\right]^{1/2}}\right] \qquad (3)$$

This resultant energy and direction is calculated for each of the energies in the pre-sheath distribution. Note that the temperature associated with the Xe II and Xe III ions which impact the surface will be less than those entering the sheath.

The sputter yield associated with each energy in the distribution is calculated using the modified Bohdansky equation which is good for heavy and light ions:[17]

$$y(E_{i,W},\theta) = \frac{0.042 Q S_n(E)}{E_S}\left(\frac{R_P}{R}\right)\left[1-\left(\frac{E_{TH}(\theta)}{E_{i,W}}\right)^{2/3}\right]\cdot \left[1-\left(\frac{E_{TH}(\theta)}{E_{i,W}}\right)\right]^2 \quad (4)$$

The threshold energy in Eqn (4) is a function of angle of impact. For small angles (= 60 deg), the modified (reduced) threshold is simply[18]

$$E_{TH}(\theta) = E_{TH}(\theta = 0)\cos^2(\theta). \quad (5)$$

The sputtering threshold at normal incidence was taken to be 31 eV.[19]

In order to determine the number of Mo atoms sputtered, the number of Xe II and Xe III ions hitting a 1 mm^2 region along the radius of the DCA was approximated given the velocities of the ions and an estimate of the Xe II number density at the sheath. (1 mm^2 roughly corresponded to the cross-section of the LIF interrogation volume.) The number density at the sheath was approximated from LIF Xe II data[4] and from previous number density measurements near the exit of a similar DCA.[8] The number of Xe II ions per second impacting the surface was

$$N^+(r) = n^+(r) Av_w^+(r)\left[\frac{E_{PS}^+(r)}{E_W^+(r)}\right]^{1/2} \quad (6)$$

For Xe III ions, the pre-sheath number density was calculated using the ratio of doubly to singly charged ion number densities and the number impacting the wall per second was

$$N^{++}(r) = n^+(r)\frac{n^{++}}{n^+} Av_w^{++}(r)\left[\frac{2E_{PS}^+(r)}{E_W^{++}(r)}\right]^{1/2} \quad (7)$$

Based on the mean-free-path calculations, the ratio n^{++}/n^+ was assumed proportional to the ratio of current densities measured downstream of the thruster:

$$\left.\frac{n^{++}}{n^+}\right)_{\text{at DCA}} = \left.\frac{n^{++}}{n^+}\right)_{\text{at grids}} = \left.\frac{j^{++}}{2\sqrt{2}\,j^+}\right)_{\text{in plume}} \quad (8)$$

The number of sputtered atoms per unit area was the sum of the sputter yield for given ion energy multiplied by the number of impinging ions with that energy per unit area:

$$N_{Mo} = \sum_{E_{i,W}} N_{E_{i,W}}\, y(E_{i,W}) \quad (9)$$

where N_E was determined by the normalized distribution of ion velocities. The amount of sputtered material per unit area for the actual wear tests was taken from the published average erosion rates or from published cross-sections of the eroded surfaces.[1,2,3]

The ion keeper current per unit area was calculated from the number of ions striking the keeper downstream surface. The total current was calculated using annular area for each radial position. Current to the outer (cylindrical) surface of the keeper and to the keeper flange at the back of the discharge chamber was assumed to be negligible.

A second prediction of DCA erosion was based on LIF measurements of Mo along the face of a keeper over a range of thruster operating conditions.[4] Sensitivities for the erosion are estimated to be 13 μm/khr/A and 25 μm/khr/V given a 63 μm/khr rate for 13.1 A, 25 V reference point. While the 30 cm data should lend itself directly to this correlation, 40 cm data may not due to the use of a radically different DCA. As a first approximation, the voltage dependence is assumed to be the same, but the current dependence is taken about a 26 A datum since the cathode orifice diameter is roughly twice as large. Predictions of erosion rates based on these sensitivities and discharge operating conditions are referred to as "LIF predictions" in the following analysis and discussion.

Screen Grid Erosion

One prediction of screen grid erosion used a formulation of V. Rawlin.[14] It is an estimation of the peak screen grid erosion based on experimental and expected values of beam current, screen grid current, discharge voltage, and j^{++}/j^+.

The beam current is a sum of the Xe II and Xe III currents:

$$J_B = J^+ + J^{++} \quad (10)$$

In terms of current density, Eqn (10) becomes

$$\frac{1-\phi}{\phi} J_B A_{SG} = j^+ \left(1 + \frac{j^{++}}{j^+}\right).$$

Rearranging and including the flatness parameter, F, and the centerline correction factor of 1.4 yields an expression for j^+ on centerline:

$$j^+ = \left[\frac{(1-\phi)}{\phi}\right] J_B \left[FA_{SG}\left(1 + 1.4\frac{j^{++}}{j^+}\right)\right]^{-1} \quad (11)$$

The centerline doubly charged ion current density is simply

$$j^{++} = 1.4\left(\frac{j^{++}}{j^+}\right)_M j^+ \quad (12)$$

where $(j^{++}/j^+)_M$ is the integrated (i.e. measured) value. The screen grid erosion rate is

$$R_{Screen} = \left(j^+ y^+ + \frac{j^{++} y^{++}}{2}\right)\frac{M}{N_A \rho} \quad (13)$$

Incorporating Eqs. (11) and (12) into Eq. (13) yields

$$R_{Screen} = \frac{\left[\frac{(1-\phi)}{\phi}\right] J_B \left(y^+ + 0.7\frac{j^{++} y^{++}}{j^+}\right)\frac{M}{N_A \rho}}{\left[FA_{SG}\left(1 + 1.4\frac{j^{++}}{j^+}\right)\right]} \quad (14)$$

A modified version of the DCA erosion model provided another means of predicting screen grid erosion rates and a means of increasing confidence in the DCA model. This model was identical to the DCA model with the following exceptions: the pre-sheath velocity was taken as the Bohm velocity, the number density at the screen grid was calculated from the peak beam current and from the discharge voltage, and the calculation was carried out at a single point instead of across a radius. This predicted the grid erosion on centerline which has been shown to be the site of greatest erosion on the grid.[1,3] The ion temperature is assumed to be the same at the screen grid as it was near the DCA. Table 2 compares the erosion rates predicted by the two models to those measured following different tests. Note the close agreement of both models to the measured values. In addition, the predictions of relative contributions of Xe II and Xe III to the screen grid erosion agreed to within 0.1 percent.

Results

Figure 3 compares j^{++}/j^+ ratios measured in the plume of the 30 cm diameter thruster (EMT 4) to those measured previously as a function of discharge current. FT 1 is the first of two NSTAR flight engines which was tested at both GRC and JPL. The Pathfinder engine was the immediate precursor to the flight engines. EMT 2 was the thruster used in the LDT at JPL. The EMT 4 data were consistently higher than the majority of the data at each J_D but still within the spread of data.

Screen grid and DCA keeper erosion rate predictions are also given in Fig. 3. The two models of screen grid erosion were in good agreement, differing by at most 20 percent at the highest beam/discharge current. LIF Mo erosion rate data[4] are included in Fig. 3 and agree well with the keeper model of the erosion. The LIF prediction based on sensitivities from the LIF analysis also are in good agreement.

Figures 4 and 5 illustrate the variation in j^{++}/j^+ with 40 cm thruster discharge current and voltage, respectively. These indicate relative j^{++}/j^+ sensitivities of 0.015 A^{-1} and 0.05 V^{-1} respectively for reference values of 22 A and 26 V. From Fig 5, the discharge voltage dependence of the ratio is similar to that for the 30 cm thruster. The EMT operation was at its nominal 1.76 A beam current condition. The 40 cm LMT is operated at the same beam current density (3.52 A).

Figures 6 and 7 provide additional comparisons between the 30 and 40 cm thrusters (also at respective beam currents of 1.76 and 3.52 A) in terms of doubly charged ion production as a function of discharge propellant efficiency. Note that j^{++}/j^+ increased proportionally to beam ion production cost. The predictions of screen grid erosion rates were again in good agreement, especially for EMT operation. The error bars reflect uncertainties in j^{++}/j^+. Xe II appears to contribute less than 5 percent to the erosion during 25 V (V_D) operation.

Predictions of the DCA erosion model were consistently higher than those based on LIF sensitivities. Both, however, were only indications of the relative rates as number densities near the keeper are not well known.

Centerline number densities were assumed to be on the order of 10^{13} cm^{-3} for 13 A, 25 V, 30 cm operation given measured number densities of 3-$5{\cdot}10^{12}$ cm^{-3} for 6 A, 20 V operation. For this estimate, y^+/y was on the order 10^{-5}. The trends in Figs. 6 and 7 show remarkably similar trends suggesting the trends were general. Data at other operating conditions not reported here support this generalization.

In addition to the single point calculations made in support of j^{++}/j^+ measurements discussed above, the DCA erosion model was employed to gain a better understanding of the keeper erosion observed in the LDT. It was assumed that erosion along the inner edge of the keeper orifice resulted from back-flowing ions and not from ions moving radially outward and impacting the inner wall of the keeper orifice. This assumption was primarily motivated by the desire to compare the models predictions with observed ion energies near the downstream face of the keeper.[4,16] (No LIF data were collected in the orifice.) A combination of back-flowing and out-flowing ions is expected to actually result in the chamfering of the inner radius of the keeper.

Given the radially distributed erosion pattern at the end of the LDT,[3] Xe II energies and angles of incidence at the sheath were calculated to match the erosion rates. Average discharge voltage, current, j^{++}/j^+, and discharge keeper voltage were assumed over the entire 8.2 khr. Table 3 presents the predicted values over a range of Xe II number densities. Measured energies and angles are also presented. The calculated energies and angles for $r/r_o > 0.42$ were close to measured values for $n^+ = 5{\cdot}10^{12}$ cm^{-3}. For $r/r_o < 0.42$ the energies were less than those predicted for this density. (Note that no LIF data were taken beyond $r/r_o > 0.63$.) The energies were inversely proportional to number density, as expected. The fraction of sputtered Mo attributed to Xe II was on the order of 10^{-3} percent at $5{\cdot}10^{12}$ cm^{-3} and decreased as the number density increased. At a significantly lower than expected density of 10^{11} cm^{-3} the contribution of Xe II to the overall erosion becomes significant. As j^{++}/j^+ or the Xe II number density was decreased, the Xe II energies necessary to generate the same eroded pattern increased.
Ion currents to the keeper face were calculated to be between 0.05 and 0.1 A. These are between 25 and 50 percent of the measured ion saturation current to the keeper.[7] However, since the measurement of the saturation current may perturb the plasma structure, and the large uncertainties in the parameters leading to the predicted ion fluxes, a factor of two was considered acceptable agreement.

Figure 8 compares predicted keeper erosion patterns as a function of thruster power. (Recall that the erosion profile for the 2.3 kW operating condition was an input to the model.) NSTAR throttling conditions were assumed and n^+, V_D, and j^{++}/j^+ were varied accordingly.[11] The impinging ion energies and angles were held constant. Note that the erosion increases most rapidly with power along the inner radius and at the half radius point.

Since the erosion is Xe III dominated for these conditions, the erosion rates varied linearly with j^{++}/j^+, everything else being held constant. Increases in the cathode fall voltage preferentially increased the erosion along the inner radii. Figure 9 illustrates the change in depth after 1000 hr (NB, not the depth after 8.2 khr as given in Fig. 8) with fall voltage. The pre-sheath energies and angles again were held constant. As the keeper inner diameter increases with time, it was expected that these parameters would change and the erosion would increase. Calculation of these parameters was beyond the scope of this investigation.

Discussion

The variation in j^{++}/j^+ with ν_D was similar for the 30 and 40 cm diameter engines. The efficiency was varied at constant discharge current for the 30 cm data, as opposed to at constant discharge voltage for the 40 cm data. Note that the variation in discharge losses was also similar. The similar trends indicate that the method of variation was not a factor.

Because of the large Xe III charge exchange mean-free-path, the screen grid and DCA erosion rates followed the same trends as a function of the ratio of doubly to singly charged ion currents. Since the beam current density, discharge voltage, and screen grid open area fractions were nearly identical for the two thrusters, the screen grid erosion rates should be nearly identical. The slightly lower number of Xe III ions in the 40 cm thruster resulted in slightly smaller erosion rates. Note that both are extremely low and screen grid erosion should not be significant for ν_D on the order of 0.9.

Similarly, the DCA erosion varied slightly as a result of the lower number of Xe III ions. More accurate measurements of Xe II and Xe III densities near the DCA would significantly improve the evaluation of the DCA erosion.

The lower j^{++}/j^{+} ratio in the plume of the 40 cm thruster for the same beam current density most likely resulted from improvements in the design of the discharge chamber. Operation at a slightly lower discharge voltage (24 versus 25 V) and smaller discharge voltage oscillations decreased the number of Xe III created. The greater efficiency of the discharge is reflected in the 40 cm's lower discharge losses.

Erosion rate predictions based on the j^{++}/j^{+} ratio indicated a slightly stronger dependence on discharge voltage than on discharge current. Previous LIF investigations[4] also suggest a stronger dependence on V_D than on J_D, but emission data suggest the opposite trends.[7]

For V_D>25 V, sensitivities of j^{++}/j^{+} to discharge voltage were similar to those measured during NSTAR thruster sensitivity testing.[20] Below 25 V, the sensitivity of j^{++}/j^{+} to V_D appeared to decrease significantly for the 40 cm thruster but remained relatively constant for the 30 cm thruster. The reason for the difference in behavior is unclear.

The model predicts that small pre-sheath energies would be needed to match the erosion observed in the LDT. For these energies, the contribution of Xe II to the erosion was negligible. Both of these results are consistent with keeper erosion measurements conducted at GRC.[7] From previous Langmuir probe data[16] on a lower power hollow cathode, the n^{+} near the orifice is expected to be on the order of $5 \cdot 10^{12}$ cm^{-3}. However, there is significant uncertainty in this value and in the variation of the density across the keeper face. If the plasma structure were to vary significantly resulting in pre-sheath energies on the order of 10 eV, Xe II would contribute significantly to the observed erosion. While plasma density variations are believed to be the primary source of steady state ion acceleration, voltage fluctuations could supply energies above 10 eV in lean cathode operation. The model also predicts that the erosion pattern is very sensitive to keeper potential. However, actively controlling V_K could prove problematic.

Discrepancies between measured and predicted Xe II pre-sheath energies may result from large uncertainties in the angle of incidence for the inner radii. Note that the measured angles of the bulk Xe II velocities for $r/r_o < 0.4$ are greater than 90 degrees, i.e., the ions are moving away from the surface of the keeper. Even though these data were repeatable over the inner repeatable for keeper operation, there was a large uncertainty in the small axial components of velocity.[8] Significant charge exchange could result in these outward flowing ions which could mask a flux of ions to the surface in the wings of the outward flowing ion distribution. Mean free paths for Xe II charge exchange near the exit of the cathode were expected to be on the order of a few millimeters. Although the energies of the impacting ions were independent of the angle at which the ions entered the sheath (Eq. 2), the angle could vary the sputter yield by as much as a factor of two.[8,18] For pre-sheath energies of a few volts ions entering at 45 degrees, the angle of incidence at the keeper face would be on the order of 15 degrees, sufficient to increase the erosion by 20 percent. If the ions along the inner radii entered at small angles, the predicted energies necessary to produce the erosion would increase to around 2 eV at $n^{+} = 5 \cdot 10^{12}$ cm^{-3} which is closer to the expected Bohm energy. Also note that the sputter yield near threshold has an uncertainty of more than a factor of 2 and that a factor of two decrease in the predicted erosion rate would also result in increases in the required energies.

Throughout the erosion pattern predictions discussed above, the pre-sheath energy distribution across the face of the keeper was assumed to be independent of operating condition. (NB, the plasma density was not.) This was taken as a conservative (over-predictive) estimate of the erosion at lower discharge currents and thruster powers. LIF data indicated that the pre-sheath energies decrease with lower thruster powers, however the data was not sufficient to quantify this variation across the face of the keeper.[16]

Conclusions

The ratio of doubly to singly charged ion currents has been measured in the plume of a 30 cm EMT and of a 40 cm LMT. The ratio increased with discharge voltage for constant discharge current and with discharge current for constant discharge voltage. The ratio followed the

increase in ion production cost as a function of discharge propellant utilization efficiency. The trends in DCA and screen grid erosion for the 30 and 40 cm thrusters were similar.

A simple model of DCA keeper erosion was developed. It indicated that Xe II plays an insignificant role in DCA erosion for typical discharge chamber operating conditions. However, Xe II energies and angles of impingement measured in a previous investigation via LIF appear to accurately predict the flux of ions to the keeper assuming Xe III ions have twice the energy and the same angle of approach as the Xe II ions. The model suggested that the erosion near the inner radii was most sensitive to the cathode fall voltage. Agreement between this model and LIF data near the DCA and between a modified version of the model applied to screen grid erosion and the standard screen grid erosion model increased confidence in the DCA model's predictive capability.

A more detailed measurement of plasma properties near the DCA, especially the 40 cm DCA, is needed to develop a more sophisticated model. In addition, Xe III and Xe II LIF near the DCA and downstream of the grids would provide another means of measuring j^{++}/j^{+} with very high spatial resolution. Xe III LIF would also permit direct measurement of the pre-sheath energies and velocity vectors assumed in this investigation The diagnostic techniques required to make these measurements are under development at GRC.[21]

Acknowledgements

The authors gratefully acknowledge the fabrication and test support provided by GRC's Test Installation Division and AKIMA personnel.

References

[1] Patterson, M. J., et al, "2.3 kW Ion Thruster Wear Test," AIAA-95-2516, 31st Joint Propulsion Conference (July, 1995).

[2] Polk, J. E., et al, "A 1000-Hour Wear Test of the NASA NSTAR Ion Thruster," AIAA-96-2717, 32nd Joint Propulsion Conference (July, 1996).

[3] Polk, J. E., "An Overview of the Results from an 8200 Hour Wear Test of the NSTAR Ion Thruster," AIAA-99-2446, 35th Joint Propulsion Conference (June, 1999).

[4] Williams, G. J., *et al.* "30 cm Discharge Cathode Erosion," IEPC-01-306, 27th International Electric Propulsion Conference (October, 2001).

[5] Anderson, J. R., *et al.*, "Results of an On-Going Long Duration Ground Test of the DS1 Flight Spare Ion Engine," AIAA-99-2857, 35th Joint Propulsion Conference (June, 1999).

[6] Mantenieks, M. A., IEPC-01-309, 25th International Electric Propulsion Conference (October, 2001).

[7] Domonkos, M. T., *et al.*, "Investigation of Keeper Erosion in the NSTAR Ion Thruster," IEPC-01-308, 27th International Electric Propulsion Conference (October, 2001).

[8] Williams, G. J., *et al.*, "FMT-2 Discharge Cathode Erosion Rate Measurements via Laser-Induced Fluorescence," AIAA-2000-3663, 36th Joint Propulsion Conference, 2000.

[9] Vahrenkamp, R. P., "Measurement of Double Charged Ions in the Beam of a 30-cm Mercury Bombardment Thruster," AIAA-73-1057, 10th Electric Propulsion Conference (October, 1973).

[10] Byers, D. C., "Angular Distribution of Kaufman Ion Thruster Beams," NASA TN-D-5844, June, 1970.

[11] Rawlin, V. K., et al, "NSTAR Flight Thruster Qualification Testing," AIAA-98-3936, 34the Joint Propulsion Conference (July, 1998).

[12] Patterson, M. J>, *et al*, "Development Status of a 5/10-kW Class Ion Engine," AIAA-2001-3489, 37th Joint Propulsion Conference (July, 2001).

[13] Williams, G. J., *et al.*, "40 cm Prototype Ion Thrusters," ICOPS-P3-H02, International Conference on Plasma Science (June, 2001).

[14] Rawlin, V. K., Internal Memorandum, NASA GRC (April, 1996).

[15] Pullins, S., and R. A. Dressler, "Ion dynamics in Hall Effect and Ion thrusters," AIAA-2000-0603, 38th Aerospace Sciences Meeting (January, 2000).

[16] Williams, G. J., *et al.*, "Characterization of the FMT-2 Discharge Cathode Plume," IEPC-99-104, 26th International Electric Propulsion Conference (October, 1999).

[17] Bohdansky, J., "A Universal Relation for Sputtering and Yield of Monatomic Solids at Normal Ion Incidence," *Nucl. Instr. and Meth. In Phys. Res.*. **B2** (587) 1984.

[18] Yamamura, Y., *et al.*, "Angular Dependence of Sputtering Yields of Monatomic Solids," Report IPPJ-AM-26, Institute of Plasma Physics, Nagoya University, Japan, 1983.

[19] Mantenieks, M. A., "Sputtering Threshold Energies of Heavy Ions," IEPC-97-187, 25th International Electric Propulsion Conference(!997).

[20] Myers, R., and V. K. Rawlin, "NSTAR Thruster Sensitivity Test Review," NASA GRC Internal Memorandum (March, 1996).

[21] Domonkos, M. T., and G. J. Williams, "Status of Laser-Based Ion engine Diagnostics at NASA Glenn Research Center," IEPC-2001-304, 27th International Electric Propulsion Conference (October, 2001).

Table 1: Nominal Thruster Operating Conditions

Power (kW)	Main flow (sccm)	Cathode flow (sccm)	J_B (A)	V_B (V)	J_D (A)	V_D (V)
30 cm 1.6	14.4	2.50	1.1	1500	9.0	25.1
2.6	23.3	3.7	1.76	1500	13.1	25.0
40 cm 3.9	50.0	5.5	3.52	1050	22.2	23.9

Table 2: Comparison of peak screen grid erosion rates (μm/khr) to measured values.

	EMT 1	EMT 1b	EMT 2
Model 1 (~VKR)	41.1	7.1	10.1
Model 2 (Mod. DCA)	38.4	5.87	9.69
Measurement	38.6	5.91	-

Table 3: Comparison of Predicted and Measured Xe II Energies (eV) and Pre-sheath Angles of Bulk Velocity Along the Keeper Surface for 13 A, 25 V Operation as a function of centerline Xe II number density just downstream of the cathode.

Keeper Radius (r/r_o)	Measured Energy (eV)	10^{11} (cm^{-3})	10^{12} (cm^{-3})	$2.5 \cdot 10^{12}$ (cm^{-3})	$5 \cdot 10^{12}$ (cm^{-3})	$7.5 \cdot 10^{12}$ (cm^{-3})	10^{13} (cm^{-3})	Ang. (deg)
0.25	5.6 @ 100 deg.	11	3.2	2.0	0.9	0.6	0.5	45.
0.315	4.8 @ 120 deg.	10	3.0	1.9	0.9	0.6	0.4	45.
0.42	2.5 @ 55 deg.	10	3.5	2.1	1.0	0.6	0.5	55
0.52	-	17	5.8	3.8	2.0	1.4	1.1	50
0.63	3.7 @ 47 deg.	26	9.6	6.5	3.7	2.8	2.3	45
0.73	-	24	9.0	6.1	3.4	2.6	2.1	45
0.84	-	23	8.3	5.6	3.1	2.3	1.9	45
0.94	-	18	5.9	3.8	2.0	1.4	1.1	45
1.0	-	18	5.9	3.8	2.0	1.4	1.1	45

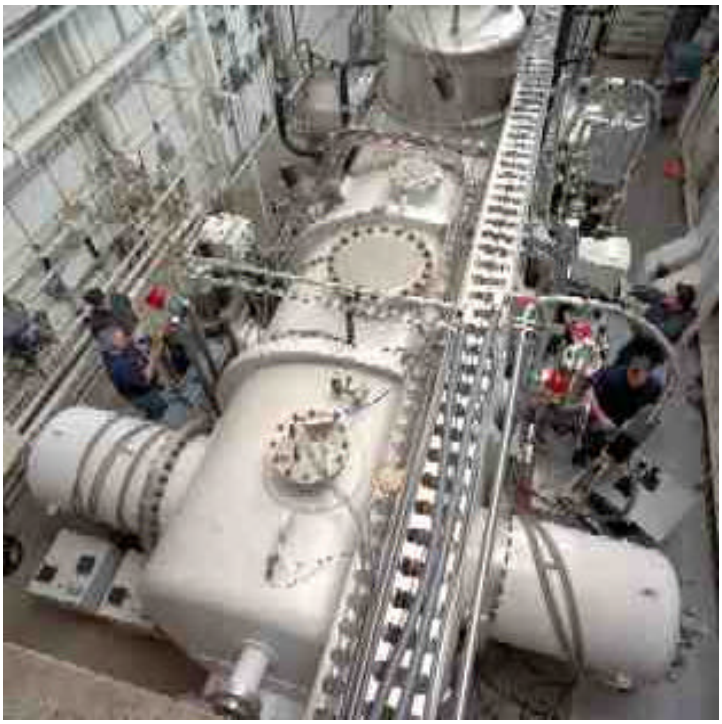

Figure 1 Vacuum facility11 at GRC. The ExB probe is located near the end of the tank in the foreground. The thruster is mounted at the opposite end of the tank.

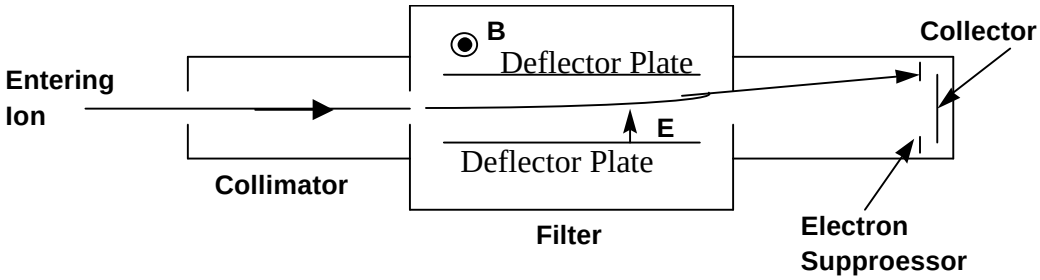

a. A diagram of velocity filtering

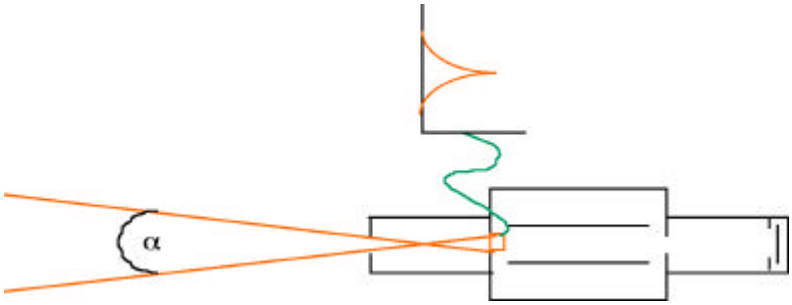

b. A diagram of signal collection showing the cross-slit variation in ion current and the acceptance angle, α.

Figure 2 Schematic diagrams of the ExB probe. The drawings are not to scale.

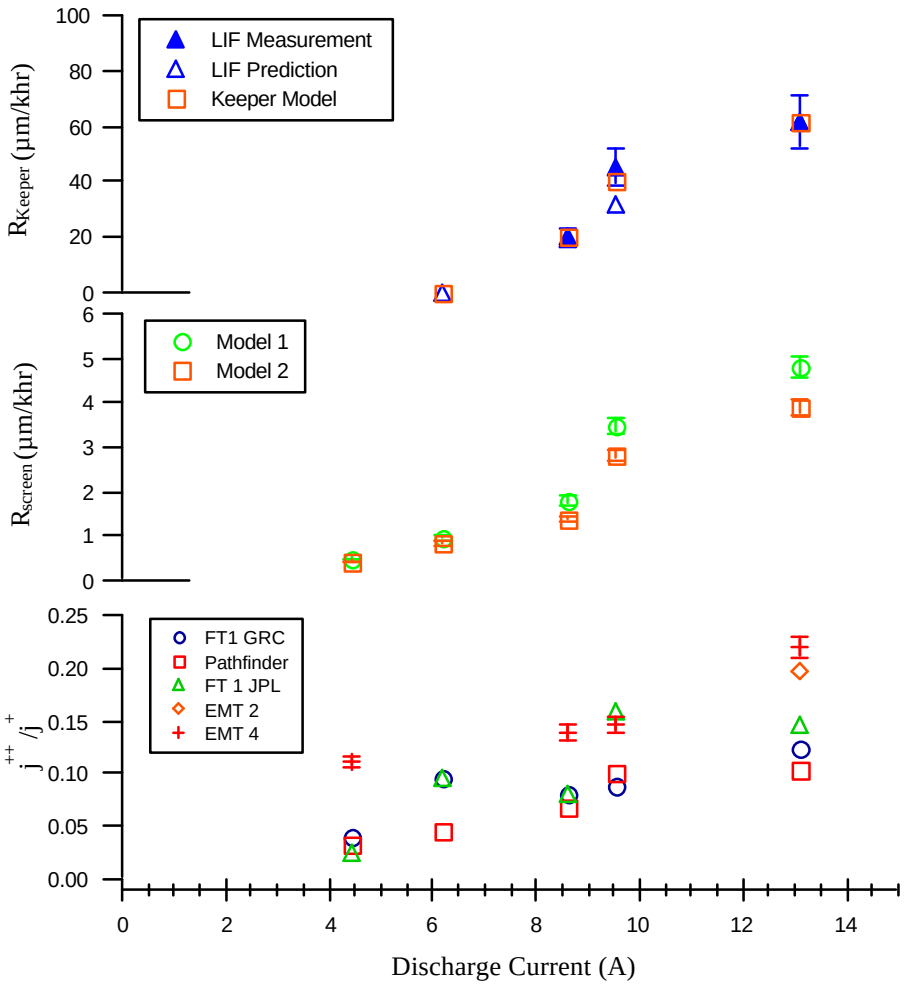

Figure 3 Variation in doubly to singly charge current ratios with discharge current. The discharge currents indicate different throttling points of the 30 cm thruster. Predictions of screen grid and DCA keeper erosion are also given.

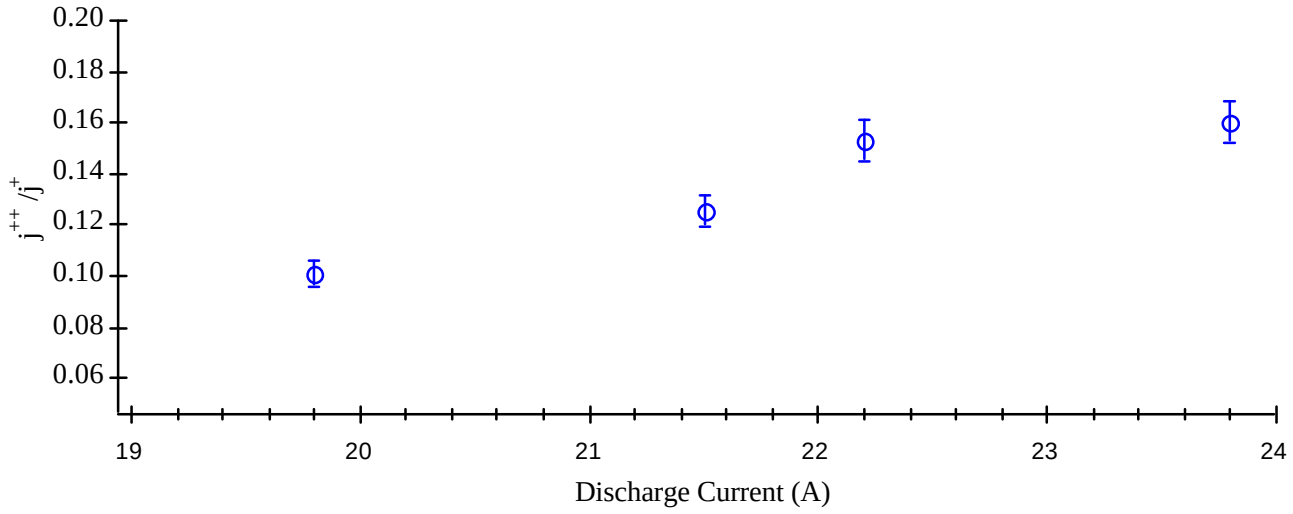

Figure 4 Variation in the doubly to singly charged current densities in the plume of the 40 cm thruster as a function of discharge current for 3.52 A J_B, 23.9 V V_D operation.

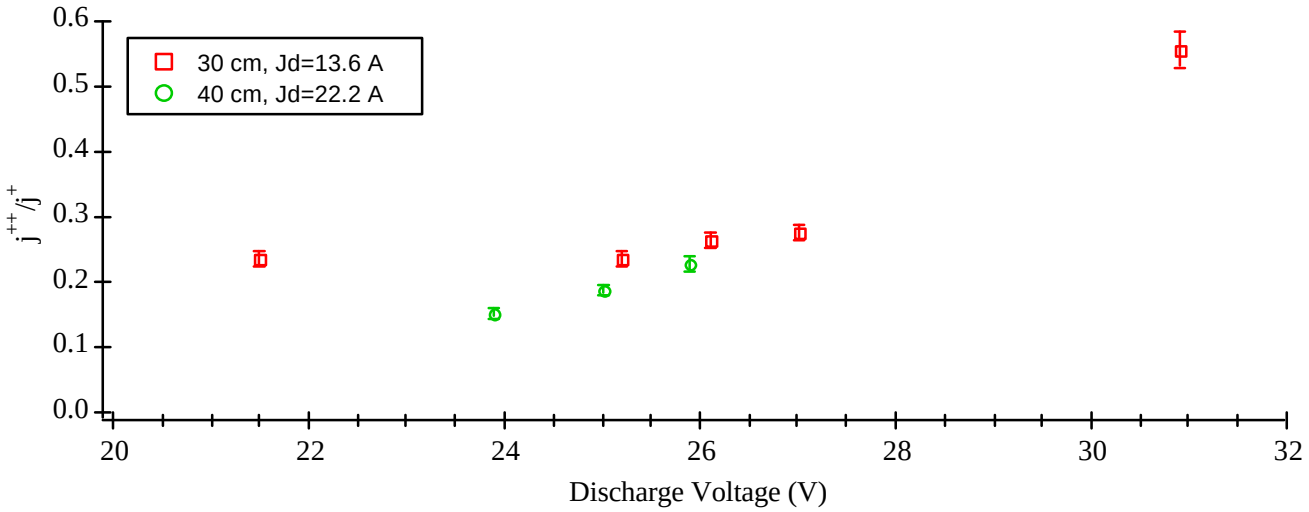

Figure 5 Variation in the doubly to singly charged current densities in the plume of the 30 cm and 40 cm thrusters as a function of discharge voltage for 1.76 and 3.52 A beam current operation respectively.

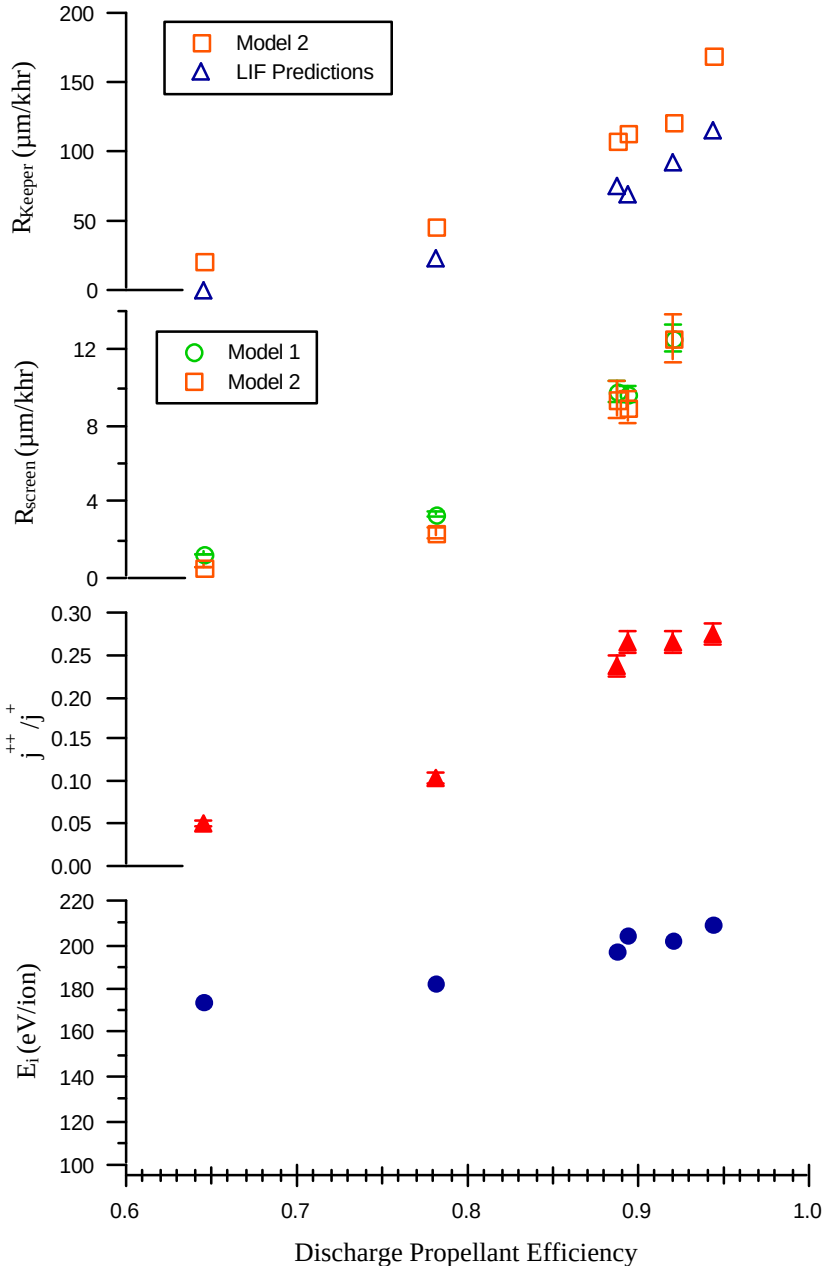

Figure 6 Variation in j^{++}/j^{+} with discharge propellant efficiency for the 30 cm EMT.

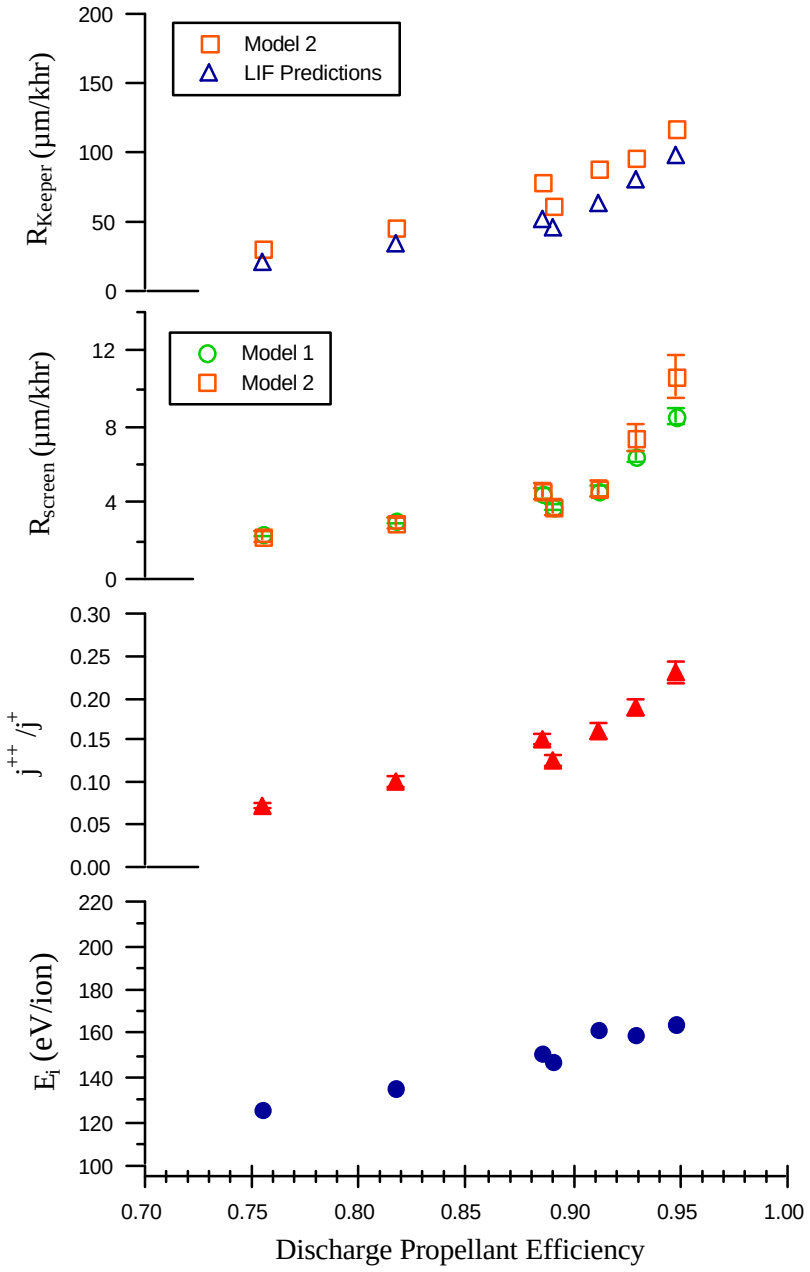

Figure 7 Variation in j^{++}/j^{+} with discharge propellant efficiency for the 40 cm LMT.

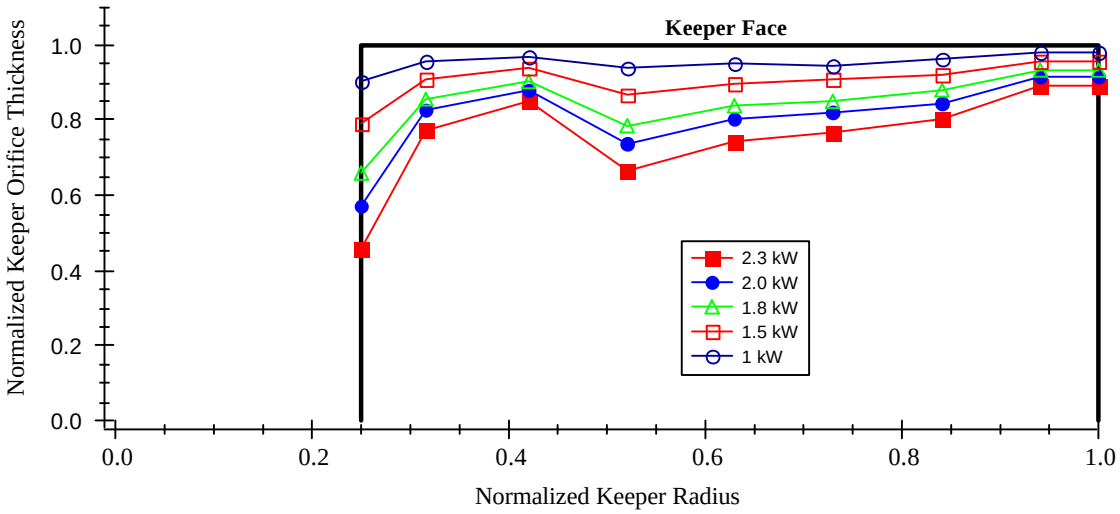

Figure 8 Comparison of predicted keeper erosion profiles as a function of thruster power. Erosion and operating conditions identical to the LDT were assumed. Pre-sheath Xe II energies and angles of incidence were calculated to match the LDT erosion at 8.2 khr.

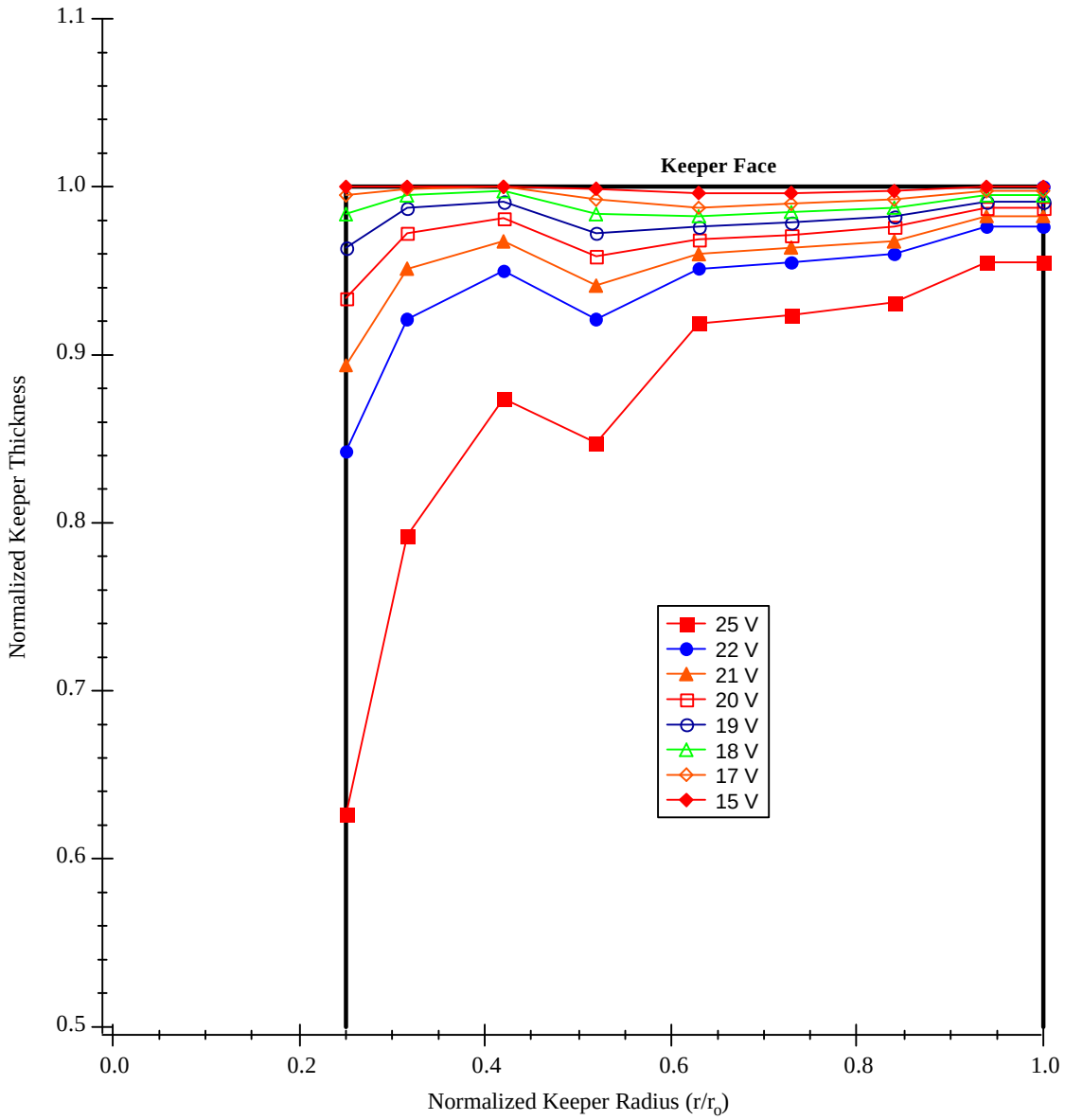

Figure 9 Comparison of erosion depths after 1000 hrs assuming different cathode fall potentials.